OzNet: A New Deep Learning Approach for Automated Classification of Covid-19 Computed Tomography Scans

Oznur Ozaltin[1], Ozgur Yeniay[1], Abdulhamit Subasi[2,3]
[1]Department of Statistics, Institute of science, Hacettepe University, Ankara, Turkey.
E-mail: oznurozaltin@hacettepe.edu.tr
E-mail: yeniay@hacettepe.edu.tr
[2]Institute of Biomedicine, Faculty of Medicine, University of Turku, 20520, Turku, Finland.
E-mail: abdulhamit.subasi@utu.fi
[3]Department of Computer Science, College of Engineering, Effat University, Jeddah, 21478, Saudi Arabia.
E-mail: absubasi@effatuniversity.edu.sa

Abstract

Coronavirus disease (COVID-19) is spreading rapidly around the world. Therefore, the classification of Computed Tomography (CT) scans alleviates the workload of experts, whose workload increased considerably during the pandemic. Convolutional Neural Networks (CNN) architectures are successful for the classification of medical images. In this study, we have developed a new deep CNN architecture, called as OzNet. Moreover, we have compared it with pre-trained architectures namely AlexNet, DenseNet201, GoogleNet, NASNetMobile, ResNet-50, SqueezeNet, and VGG-16. Additionally, we have compared the classification success of three pre-processing methods with raw CT scans. We have not only classified the raw CT scans, but also, we have performed the classification with three different pre-processing methods, which are Discrete Wavelet Transform (DWT), Intensity Adjustment, and gray to color RGB (Red, Green, Blue) image conversion on the datasets. Furthermore, it is known that the architecture's performance increases with the use of DWT pre-processing method rather than using the raw dataset. The results are extremely promising with the CNN algorithms using the COVID-19 CT scans processed with the DWT. The proposed DWT-OzNet has achieved a high classification performance over 98.8% for each calculated metrics.

Keywords: COVID-19 CT scans, Classification, CNN, 2D-DWT, Intensity adjustment.

1. Introduction

World health organization (WHO) reported that there were 149.910.744 confirmed cases of coronavirus (COVID-19), including 3.155.168 deaths in 30 April 2021 [1] from the date COVID-19 announced as a pandemic worldwide on 11.03.2020 [2]. There is more than one method for diagnosing the COVID-19. One of them is a viral test and the other is a blood test and the other is an imaging device. The most reliable of these tests is the imaging device results including chest computed tomography (CT). CT is strongly distinguished patients with COVID-19 from others. However, imaging devices are manually examined one by one by radiology experts. Considering the increasing number of cases and hospitalization rates, the workload of the relevant experts is unpredictable. Under all these conditions, it is inevitable to reduce the workload of experts with smart devices.

Image processing, video processing, etc. are performed automatically thanks to deep learning algorithms. Particularly, many studies obtained perfect results on medical image

analysis using deep learning algorithms. Wang et al.[2] merged graph convolutional network (GCN) with convolutional neural network (CNN). They called FGCNet and developed its rank-based average pooling and data augmentation. This proposed architecture was a kind of deep learning network with batch normalization, dropout. The results indicated that performance metrics were over 96.56%. Aslan et al. [3], performed lung segmentation in CT images via Artificial Neural Networks (ANN). Further, they also created two architectures which were included AlexNet. Firstly, they modified AlexNet's last layers, then called modified AlexNet via transfer learning methods. Secondly, they generated a hybrid structure with Bidirectional Long-Short Term Memories (BiLSTM) layer, it was also their proposed method. They achieved a classification accuracy of 98.7%. Nayak et al. [4] compared pre-trained architectures: AlexNet, VGG-16, GoogleNet and MobileNet-V2, SqueezeNet, ResNet-34, ResNet-50, and Inception-V3 for classification of COVID-19 chest X-ray images. Also, they compared these architectures in terms of batch size, learning rate, number of epochs, and optimizer methods for proposing to best architecture with parameters. Their proposed architecture was ResNet-34 with an accuracy of 98.33%. Yang et al.[5] created an artificial intelligence-based algorithm for the diagnosis of COVID-19 from CT. They obtained an accuracy of 89% from their algorithm.

Babukarthik et al. [6] classified COVID-19 chest X-ray images with three classes using Genetic Deep Learning Convolutional Network (GDCNN). They achieved a classification accuracy of 98.84%. When they compared their using proposed method with pre-trained architectures, their method was superior to others. Fan et al.[7] proposed Inf-Net which was a COVID-19 lung segmentation network. Further, they also utilized a semi-supervised solution with Inf-Net. They obtained a sensitivity of 87% and 86.5% performed with Inf-Net and Semi-InfNet respectively. Sharifrazi et al. [8] classified CT images using a Fusion of Convolutional Network, Support Vector Machine (SVM), and Sobel filter. They obtained an accuracy of 99.02 % by using their proposed CNN-SVM with the Sobel filter. Subasi et al. [9] used pretrained CNN architectures: VGG-16, VGG-19, ResNet152-V2, DenseNet-121, Inception-V3, MobileNet-V2 and Xception for classification of COVID-19 CT scans. Additionally, they presented some CNN architectures with one layer, three layers, and four layers. They achieved an accuracy of 85.95 % with DenseNet-121. Barstugan et al. [10] applied to feature extraction methods using Grey Level Co-occurrence Matrix (GLCM), Local Directional Pattern (LDP), Grey Level Run Length Matrix (GLRLM), Grey Level Size Zone Matrix (GLSZM), and Discrete Wavelet Transform (DWT) algorithms. In the classification phase on extracted features, they utilized SVM and obtained an accuracy of 99.68% with the GLSZM method. Khan et al. [11]'s study consists of two phases. The first phase, they extracted features using a two-level DWT of CT scans. Then, they classified utilizing their proposed deep CNN. In the second phase, they determined infectious regions of CT scans using segmentation models. They obtained a Matthews correlation coefficient (MCC) measure of 98%. Vente et al.[12] used a 3D CNN in place of 2D CNN via the transfer learning method. They achieved an Area Under Curve (AUC) of 92.3% for CT scans classification. Tuan [13] used 16 pre-trained architectures for the classification of COVID 19 CT scans without data augmentation. The study indicated that the best one is DenseNet-201 which achieved an accuracy of 96.20 ±4.95% utilizing only six epochs of training.

Adebisi et al.[14] performed AlexNet, GoogleNet, and SqueezeNet for the classification of chest X-ray images via the transfer learning method. The result displayed that

AlexNet obtained an accuracy of 98.31%. Gungor [15] had a comparative on different wavelet functions for quite noisy COVID-19 CT scans. This study also examined the different wavelet functions in terms of orthogonality, filter order, and symmetry. The results exhibited that symmetric extension (sym) or Daubechies (db) function can be used to decrease the noisy COVID-19 CT scans. Taspinar et al. [16] implemented COVID 19 X-ray images for classification using VGG-19 architecture. Moreover, they modified this architecture by powerful algorithm with feature extraction: Artificial Neural Network (ANN), Support Vector Machine (SVM), and Logistic Regression (LR). Thus, they achieved an accuracy of 96.9%. Subasi et al. [17] utilized to X-Ray images for detecting COVID-19. They classified these images with various pretrained CNN architectures. Thus, they obtained that the accuracy of VGG-19 is 97.56%. Jia et al. [18] used chest X-Ray and CT images for COVID-19 diagnosis in their study. They classified five different health problems: COVID-19, Bacterial Pneumonia, Viral Pneumonia, Tuberculosis, and normal by using CNN architectures. Moreover, they modified MobileNet and ResNet. As a result, they acquired 99.6% test accuracy on chest X-Ray images and 99.3% test accuracy on CT images. Thakur and Kumar[19] utilized two different types of images dataset: X-ray and CT images. They applied CNN architecture and they got an accuracy of 99.64% for binary classification and an accuracy of 98.28% for multiclass classification. And also, Narin et al. [20], Ahuja et al. [21], Akram et al. [22], Li et al. [23], Tuncer et al. [24], and Ozsahin et al. [25] studied on COVID 19 images. Additionally, Table 1 contains recent studies in the literature.

Table 1. Recent Studies on Covid-19 detection.

Study	**Dataset**	**Classes**	**Methods**	**Metrics**
Gaour and Jain[26]	Chest X-ray images	Covid: 546 Normal: 1139 Pneumonia:1355	Uncertainty-aware CNN	97.67% Accuracy 97.99% F1-Score 98.15% Sensitivity
		Covid:127 Noncovid:500	EfficientNetB3 MonteCarlo-Dropout	99.36% Accuracy 98.02% G-Mean
Dash and Mohopatra [27]	Chest X-ray images	Covid: 147 Normal: 500 Pneumonia:600	VGG-16 Fine Tuning	97.12% Accuracy
Chakraborty et al. [28]	Chest X-ray images	Covid: 1184 Normal: 1319 Pneumonia:600	VGG-19	97.11% Accuracy 97.00% Precision 97.00% Sensitivity
Aslan et al.[29]	Chest X-ray images	Covid:219 Normal:1341 Pneumonia:1345	ANN-based segmentation DenseNet201-SVM	96.29% Accuracy 96.41% F1-Score 96.42% Sensitivity
Saad et al. [30]	CT scans	Covid:2628 NonCovid:1620	Image Segmentation based Region of	98.90% Accuracy 98.50% Sensitivity 98.92% F1-Score

	X-ray images		Interest (ROI) Method CNN	99.30% Accuracy 98.80% Sensitivity 99.30% F1-Score
Amin et al. [31]	CT scans	Dataset I: Covid:100 Noncovid:200	Sematic Segmentation using Deeplabv3 and ResNet-18	86.47% Accuracy
		Dataset II: Covid: 349 Noncovid:701	Stack Sparse Auto-encoder (SSAE) method	100% Accuracy
		Dataset III: Covid: 1500 Noncovid: 1200		99.23% Accuracy
		Dataset IV: Covid: 10		96.15% Accuracy

In this study, we utilize Computed Tomography (CT) scans having binary classes: COVID, non-COVID. Further, we classify raw CT scans dataset using CNN architectures. Although pre-processing methods are avoided in most of the studies, we emphasize that pre-processing methods especially DWT should be used before classification, in this study. Moreover, we also put forward a new deeper CNN architecture, called as OzNet. Additionally, we compare OzNet with pre-trained architectures: AlexNet, DenseNet201, GoogleNet, NASNetMobile, ResNet-50, SqueezeNet, and VGG-16. Finally, we indicate overly being well the classification DWT-OzNet hybrid algorithm for COVID-19 diagnosis. In a nutshell of the main contributions of this study are the following:

- New framework is proposed to detect Covid-19 from CT scans with deep learning approach.
- Pre-processing methods, namely Discrete Wavelet Transform (DWT), Intensity Adjustment, and Gray to Color RGB are used to improve the performance of the classification.
- A new CNN architecture, named OzNet is developed and compared with AlexNet, DenseNet201, GoogleNet, NASNetMobile, ResNet-50, SqueezeNet, and VGG-16.

In the rest of the study, we introduce the material and methods in the next section. Then, we exhibit the results for each experiment and discuss the results in the third section. Finally, we conclude the study in the fourth section.

2. Material and Methods

In this section, first, we give details of the dataset. In the second part, we introduce some Pre-processing methods, namely Discrete Wavelet Transform (DWT), Intensity Adjustment, and Gray to Color RGB. In third part, we introduce the pre-trained CNN architectures: AlexNet[32], DenseNet201[33], GoogleNet [34], NASNetMobile [35], ResNet-50 [36], SqueezeNet [37], and VGG-16 [38]. We also present our OzNet [39] for classification CT scans. Fig.1 demonstrates the framework for the classification of CT scans.

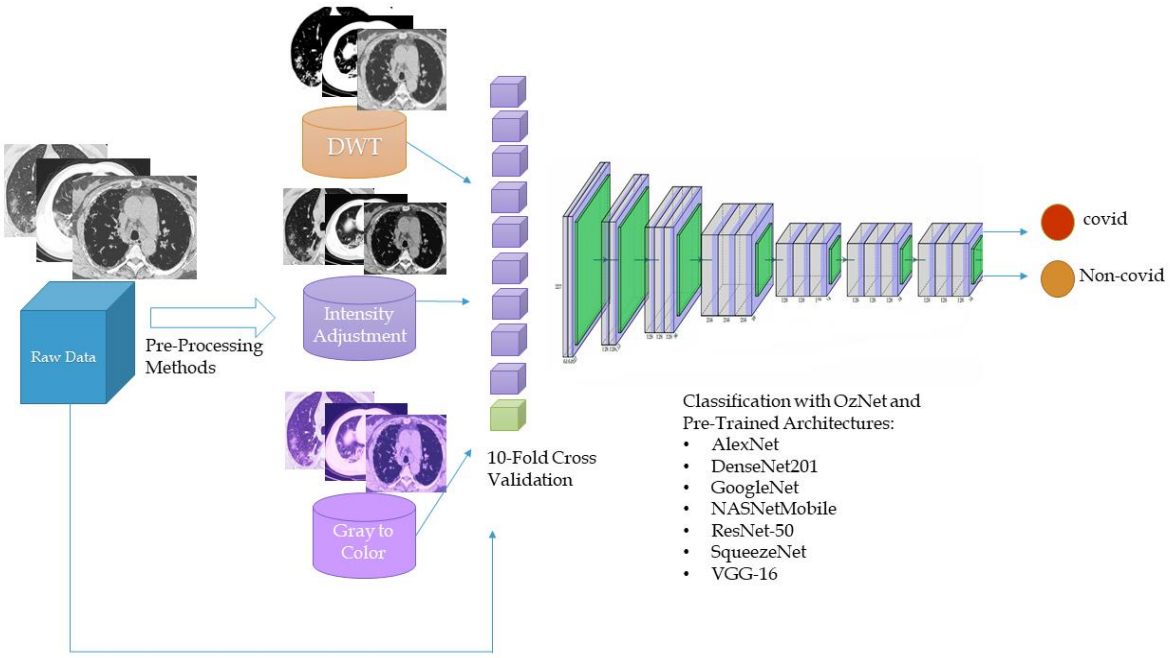

Fig1. Framework for the classification of CT scans.

2.1. CT Scans Dataset

In this study, we utilize publicly available Computed Tomography (CT) dataset for automatic classification of COVID-19. The dataset has two classes: 349 CT scans for COVID and 397 CT scans for Non-COVID [5, 40]. 349 CT scans include clinical findings of COVID-19 from 216 patients [40]. The benefit of this dataset is approved by a veteran radiologist in Tongji Hospital, Wuhan, China, who implement diagnosis and treatment of a large number of COVID-19 patients during the epidemic of this disease between January and April [40]. Fig.2 shows one CT scan image and the histogram graph with the gray channel.

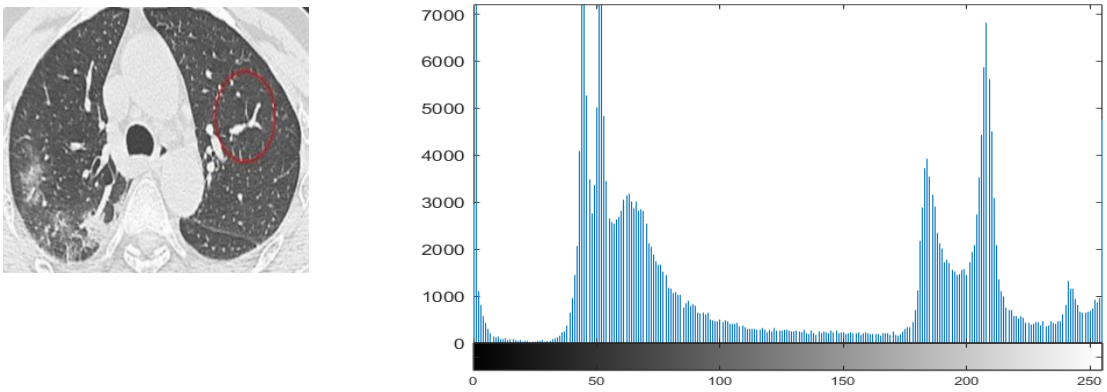

(a) (b)

Fig.2. (a) Raw CT scan image. (b) Histogram of the CT scan image.

2.2. Discrete Wavelet Transform

The wavelet transform (WT) is extensively performed in noisy images to decrease the noise [15]. 2D Discrete Wavelet Transform [41] of a CT image is given in Fig.3 (a). In WT, especially image processing, DWT is generally preferred because of the computational difficulty of Continuous Wavelet Transform (CWT) [42]. Moreover, it seizes knowledge about both place and its frequency [43].

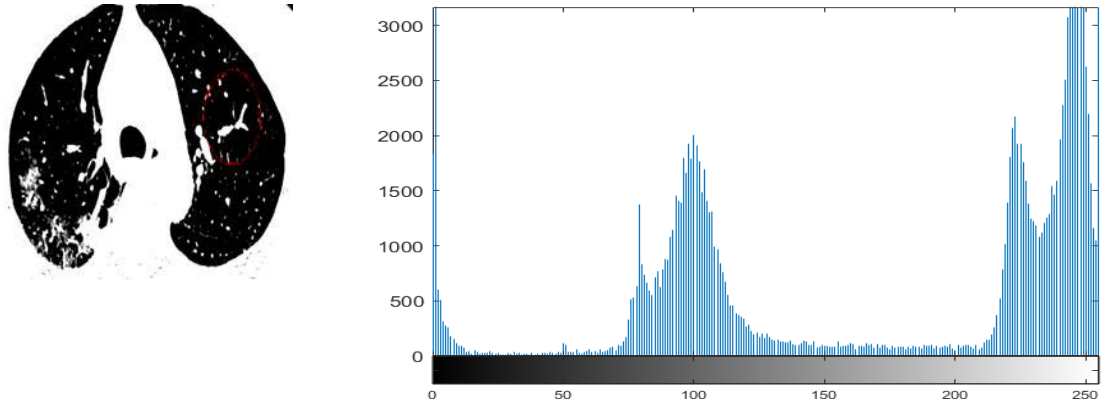

(a) (b)

Fig.3. (a) CT scan image processed with single level DWT. (b) The histogram of the DWT-CT scan image.

Calculating the wavelet coefficient at every possible scale will significantly increase the workload. To prevent this situation from occurring, groups of certain scales are formed. Mathematically, it is not different from CWT. Scale and translation parameters are usually taken as powers of two. Boundaries may vary depending on the analyst's preference. Equation 1 and equation 2 show DWT generally formula and wavelet function, respectively.

$$DWT(m,n) = \langle f, \psi_{m,n} \rangle = a_0^{-\frac{m}{2}} \sum_{-\infty}^{+\infty} f(k) \psi^* \left(a_0^{-m} k - n b_0 \right) \tag{1}$$

$$\psi_{m,n}(k) = a_0^{-\frac{m}{2}} \psi \left(a_0^{-m} \left(k - n b_0 a_0^{m} \right) \right), \quad m, n \in \square \tag{2}$$

In equation 2, a_0^m, $(a_0 > 1)$ is expressed as scale parameter, $nb_0a_0^m$, $(b_0 > 0)$ is expressed as translation parameter. To determine the time-frequency locations well $a_0 = 2$, $b_0 = 1$ is taken in the mother wavelet function, as following in equation 3 [44, 45]:

$$\psi_{m,n}(k) = 2^{-\frac{m}{2}} \psi\left(2^{-m}k - n\right), \quad m, n \in \mathbb{Z} \tag{3}$$

In this study, we apply DWT using Daubechies (dB) or Haar kernel to decrease the noise of CT scans. DWT decompose an input scan into four subgroups: Low-Low (LL), Low-High (LH), High-Low (HL), and High-High (HH). We implement single-level decomposing via the symmetric extension (sym) in light of Gungor's [15] study. Because he expressed that sym or dB function can be chosen to decline the noise of images in the study. Finally, the merging of scans is reinstatement via Inverse DWT [43]. Fig .4. shows phases of implemented DWT on COVID-19 CT scan.

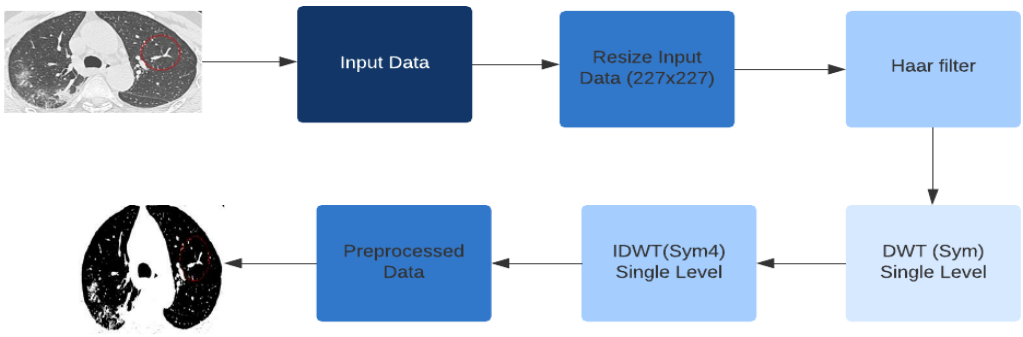

Fig.4. Phases of DWT on COVID-19 CT scans

2.3. Intensity Adjustment

Intensity Adjustment is one of the well-known contrast enhancement techniques [46]. It is improved to boost image qualification [47]. This technique is mapped low-input to low-output and high-input to high-output linearly. Further, this technique is accepted as gamma correction algorithm arguments. Based on the value of gamma, the input and output images can be nonlinearly mapped. The value of gamma can determine the contrast of images. Namely, when the gamma is taken 1, it is mapped linearly. When the gamma is taken less than 1, it is mapped nonlinearly and also has brighter output values. When the gamma is taken larger than 1, it is mapped nonlinearly and has darker output values [48]. Fig. 5 shows graphs for gamma <1, gamma=1 and gamma >1. In this study, we use this intensity adjustment technique for gamma (2 in our case), as shown in Fig. 6.

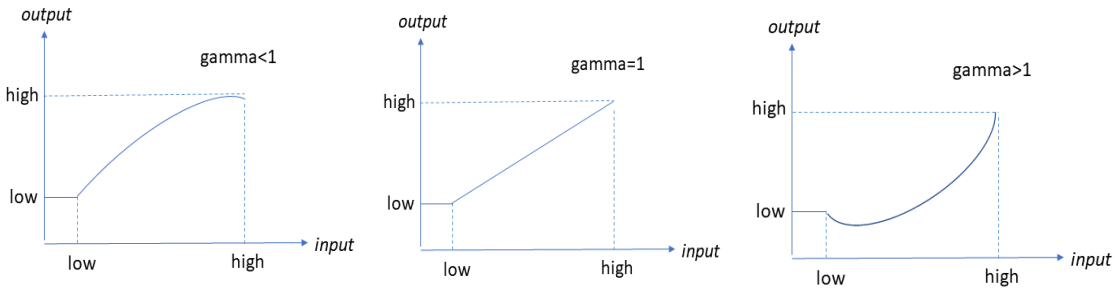

Fig.5. Graphs of the gamma values

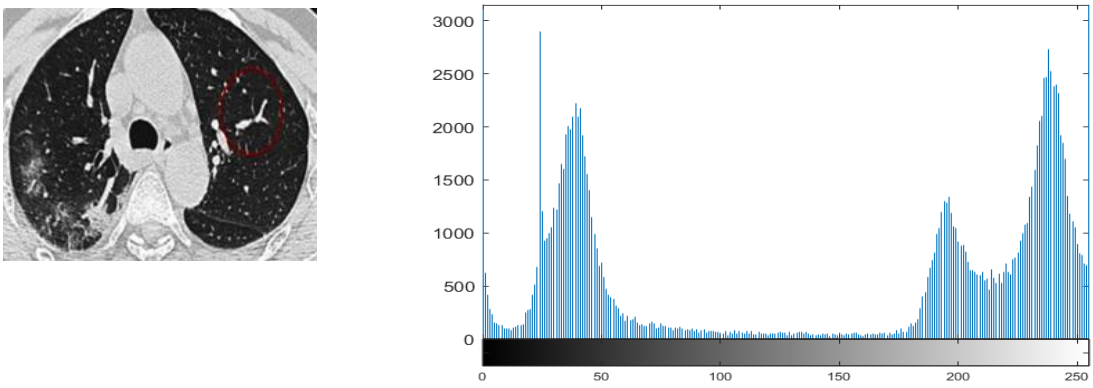

(a) (b)

Fig.6. (a) CT scan image processed with intensity adjustment for gamma 2. (b) The image histogram of the Intensity Adjustment-CT scan.

2.4. Gray to Color RGB

Gray to color RGB transform is a very important one of visualization method in image processing. It can be said that especially black and white biomedical images cannot be easily understood by the human eye [49]. This transformation generally purposes to decrease human efforts, such as a doctor, radiologist, and the other [50]. In literature, many different colors of space are used. In this study, we implement RGB color space. Since in many studies, blue-green or red-orange coloring studies were carried out, so we use purple coloring in this study. Moreover, we also perform maximum-minimum normalization to reduce the noise and resized 227x227 of the CT scan images. Fig.7 shows one of the transformed colors RGB CT scan image and its histogram.

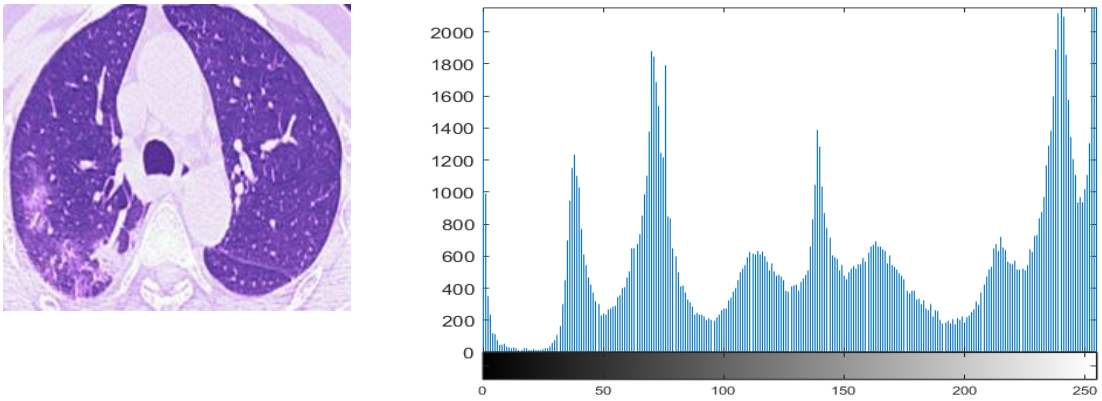

(a) (b)

Fig.7. (a) CT scan image processed with gray to color RGB. (b) The histogram of the color RGB-CT scan.

2.5.Pre-Trained CNN Architectures

Thanks to the end-to-end structure of deep learning algorithms that continue to develop day by day, these algorithms are widely used in classifying medical images. Convolutional neural networks (CNN) are one of the deep learning algorithms that are well-known and widely used in image processing. The CNN architecture was presented LeNet [51] firstly. Diverse architectures were grown since then, such as AlexNet [32], DenseNet201 [33], GoogleNet [34], NASNetMobile [35], ResNet-50 [36], SqueezeNet [37], and VGG-16 [38]. It takes a lot of time to develop robust architecture at CNN, so using pre-trained architectures is highly advantageous. Further, we also develop one of the deep learning architectures called OzNet [39] and compare it to these well-known architectures. We select AlexNet, DenseNet201, GoogleNet, NASNetMobile, ResNet-50, SqueezeNet, and VGG-16 because of tried many times and being famous architectures. The structure of these architectures is briefly described below.

AlexNet [32] has five convolution layers with a merge of max-pooling layers, three fully connected layers, two dropout layers, and a softmax. Moreover, each layer is activated with the ReLU activation function. The total number of parameters is 62.3 million. By default, the input image size is 227x227x3.

DenseNet201 [33] has 201 deep layers. In DenseNet201, each layer is related to all previous layers. When creating feature maps, they merge and forward them to the next layer. Traditional CNN architectures have L layers and L connections. Here, the architecture with L layers has L(L+1)/2 connections. Thus, it is a CNN architecture with strong memory that can compute with high efficiency. The total number of parameters is nearly 20 million. By default, the input image size is 224x224x3.

GoogleNet [34], has 22 layers deep with two convolution layers, four max-pooling layers, nine inception layers, a global average pooling layer, a dropout layer, a linear, and a Softmax. Further, each convolution inside is activated with the ReLU activation function. The total number of parameters is seven million. By default, the input image size is 224x224x3.

NASNetMobile [35] targets finding optimum CNN architecture via the Reinforcement learning technique. Neural Architecture Search (NAS) was developed by the Google Brain team [52]. There are different sizes of NAS architectures. NASNetMobile is a reduced version. The total number of parameters is nearly 4.5 million. By default, the input image size is 224x224x3.

ResNet50 [36] has 48 convolution layers, one max-pooling layer, and one average pooling layer. In total, it consists of fifty layers deeper. It is not a classical CNN architecture because of has residual blocks. Thus, thanks to its ability to reduce the weights on the layers by half, it is among the robust architectures. The total number of parameters is over 23 million. By default, the input image size is 224x224x3.

SqueezeNet [31] has 2 convolution layers, eight fire modules, three max-pooling layers, an average-pooling layer, and a Softmax. The total number of parameters is 1.24 million. By default, the input image size is 227x227x3.

Very Deep Convolutional Networks for large-scale Image Recognition namely VGG-16 [32] have thirteen convolution layers, five max-pooling layers, three fully connected layers, and a Softmax. Additionally, each hidden layer is activated with the ReLU activation function. The total number of parameters is 138 million. By default, the input image size is 224x224x3.

In any CNN architecture, image feature extractions occur in the first layer, so the initial learned phase starts in this layer. Hence, in this study, the first layer is not any altered. However, the last layer can be altered to receive highly advantage in a CNN architecture. When transfer learning methods are utilized, beforehand learned parameters are taken their place in the new CNN architecture [3]. In this study, we replace the last layers with new layers for selected pre-trained architectures.

In this study, we compare OzNet with well-known architectures: AlexNet, DenseNet201, GoogleNet, NASNetMobile, ResNet-50, SqueezeNet, and VGG-16. Consequently, for a fair comparison, we apply the same option parameters for each architecture during training progress. In this study, we determine the having best values option parameters with trial and error. The option parameters are detailed in Table2.

Table 2. Options parameters for each CNN architecture

Parameter	**Value**
Optimization Methods	sgdm
Momentum	0.90
Constant Initial Learn Rate	0.0001
Gradient Threshold Method	L2norm
Max Epochs	10
Mini Batch Size	8
Shuffle	Every-Epoch
L2 regularization	0.0001

2.6. New Deep Learning Approach: OzNet

In this study, we present a new deep learning architecture, called as OzNet. This architecture has 34 layers which are seven convolution layers, seven max-pooling layers, seven batch normalization layers, seven ReLU activation layers, two fully connected layers, one dropout layer with 0.5 probability, one SoftMax layer, and one classification layer using cross-entropy approach. We aim to prepare an architecture consisting of seven blocks, each block is included a convolution layer, a normalization layer, an activation layer, and a max-pooling layer as shown in Fig.8. The convolution layers of each block are employed for feature extraction from the CT scan dataset. While the dimension of the images is reduced in each block, it is also filtered from noise. Of course, each block does not have the same number of filters, padding, and stride. Layer parameters are detailed in Table 3. Notably, we should emphasize that these layer parameters have been tried many times to find the architecture making the best classification. Additionally, this architecture is not only used on this COVID-19 CT scan dataset. It is also tried on another dataset [39, 53] and it has been found to be successful again.

Additionally, we implement 10- fold cross-validation for trustful results. Furthermore, we utilize data augmentation on raw and pre-processed CT scan datasets to overcome extreme learning from datasets.

2.7.Data Augmentation

In this study, we apply data augmentation on raw and pre-processed CT scan datasets. Although we resize the dataset before pre-processing methods, we deem it suitable for data augmentation. Because each architecture's appropriate input size is different from the other and the number of images is not enough for the best training. Thus, we reduce over-fitting when applying data augmentation. We utilize shearing, reflection, and rotation data augmentation options, in this study. The horizontal shear range which is randomly chosen from a continuous uniform distribution and applied as [-0.05,0.05]. Identically, the vertical shear range which is also randomly chosen from a continuous uniform distribution and applied as [-0.05,0.05]. Random reflection is taken as 1 probability. The random rotation is applied as [-5,5] in both horizontal and vertical ranges.

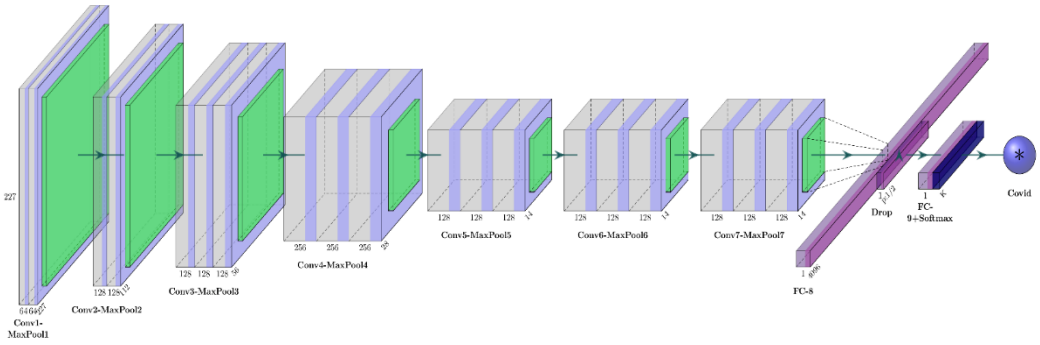

Fig.8. *New Deep Learning Approach: OzNet Scheme*

Table 3. OzNet parameters details.

Layer Name	*Type*	*Filter Size*	*Number of filters*	*Stride*	*Padding*	*Activation*	*Output Size*
Input	Image Input						227x227x3
Conv-1	Convolution 2D	64	5x5	1	1	ReLU	225x225x64
MaxPool-1	Max Pooling		3x3	2	0	-	112x112x64
Conv-2	Convolution 2D	128	3x3	1	1	ReLU	112x112x128
MaxPool-2	Max Pooling		3x3	2	0	-	55x55x128
Conv-3	Convolution 2D	128	13x13	1	0	ReLU	55x55x128
MaxPool-3	Max Pooling		3x3	2	0	-	27x27x128
Conv-4	Convolution 2D	256	7x7	1	1	ReLU	27x27x256
MaxPool-4	Max Pooling		2x2	2	0	-	13x13x256
Conv-5	Convolution 2D	128	3x3	1	1	ReLU	13x13x128
MaxPool-5	Max Pooling		3x3	2	0	-	6x6x128
Conv-6	Convolution 2D	128	3x3	1	1	ReLU	6x6x128
MaxPool-6	Max Pooling		3x3	2	0	-	3x3x128
Conv-7	Convolution 2D	128	3x3	1	1	ReLU	3x3x128
MaxPool-7	Max Pooling	-	2x2	2	0	-	1x1x128
FC-8	Fully Connected	4096					1x1x4096
Drop-8	Dropout	50%					
FC-9	Fully Connected	3 (number of class)					1x1x3
Softmax	Softmax						1x1x3
Output	Classification	Cross entropy					

3. Results and Discussion

Cross-validation is a very trustful method for classification when the data is limited. The dataset is split randomly with the determined number of the same dimension fold [54]. Considering one of the sub-folds as the test fold, it trains the framework with left behind folds. This transaction is iterated up to a number of folds is tested in the framework [55]. In this study, we have applied 10- fold cross-validation.

3.1. Performance metrics

In this study, we evaluate OzNet and the pre-trained architectures in terms of performance metrics which are accuracy, sensitivity, specificity, precision, F1-Score, and Geometric Mean (G-mean) as follows in Equation (4-9) [8]:

$$Accuracy = (TP + TN)/(TP + TN + FP + FN) \tag{4}$$

$$Sensitivity = TP/(TP + FN) \tag{5}$$

$$Specificity = TN/(TN + FP) \tag{6}$$

$$\Pr ecision = TP/(TP + FP) \tag{7}$$

$$F1 - Score = (2 \times TP)/(2 \times TP + FP + FN) \tag{8}$$

$$G - Mean = \sqrt{Sensitivity \times Specificity} \tag{9}$$

here, TP: True Positive, FP: False Positive, TN : True Negative, and FN: False Negative is presented.

3.2. Experimental Results

In this study, we utilize pre-trained architectures which are AlexNet, DenseNet201, GoogleNet, NASNetMobile, ResNet-50, SqueezeNet, VGG-16, and OzNet in MATLAB environment with Intel Core i7-7500U CPU, NVIDIA GeForce GTX 950M,16 GB RAM, 64-bit Operating System. Also, we investigate the COVID-19 CT dataset in four different cases before the classification phase. In the first case, the dataset is used in raw form without processing. In the second case, the dataset is processed with DWT and sized 227x227 .jpg format. In the third case, the dataset is processed with intensity adjustment and again sized of 227x227 .jpg format. In the last case, the dataset is normalized min- max normalization and transformed from gray to color RGB with 227x227 .jpg format. Fig.9 shows an example of raw and pre-processed datasets. In the next step, 10-fold cross-validation is applied to all prepared COVID-19 CT datasets. Thus, we ensure the reliability of the study. Moreover, we train the pre-trained architectures and OzNet using data augmentation which options random rotation [-5,5], reflection 1, and shear [-0.05,0.05]. In this way, we obstruct overfitting when training the datasets. As a result, we acquire classification performance metrics results for each used architecture, detailed in Table 4, Table 5, Table 6, and Table 7.

a. **b.**

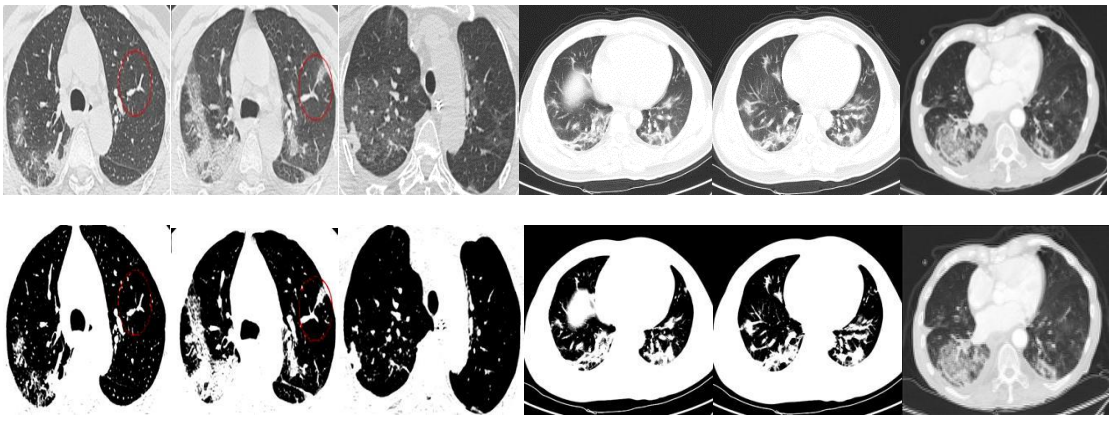

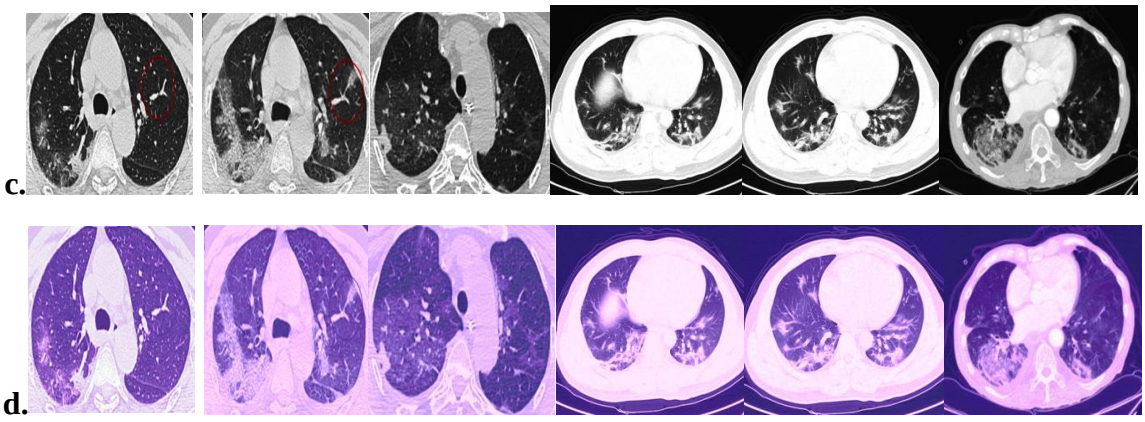

Fig.9 (a) Raw CT scan images, (b) DWT-CT scan images, (c) Intensity adjustment- CT scan images, (d) Gray to color RGB-CT scan images.

When we compare the performance of AlexNet, DenseNet201, GoogleNet, NASNetMobile, ResNet-50, SqueezeNet, VGG-16, and OzNet in terms of the raw COVID-19 CT dataset, we see that the best performance has DenseNet201 with an accuracy of 86.86 %. It has also a sensitivity of 89.69%, specificity of 84.38 %, F1-score of 86.46%. Besides, OzNet has AUC, accuracy, sensitivity, specificity, precision and F1-score which are 87.12%,78.82 %,77.36%, 80.1%, 77.36% and 77.36% respectively. All performance metrics results are demonstrated in Table 4.

Table 4. Performance metrics of CNN architectures using the COVID-19 CT dataset of raw

CNN Architectures	Performance Metrics						
	Sensitivity	**Specificity**	**Precision**	**F1-Score**	**G-Mean**	**Accuracy**	**AUC**
AlexNet	0.64756	0.81612	0.75585	0.69753	0.72697	0.73727	0.80540
DenseNet201	0.89685	0.84383	0.83467	0.86464	0.86993	0.86863	0.94890
GoogleNet	0.80229	0.82620	0.80229	0.80229	0.81416	0.81501	0.89020
NASNetMobile	0.77077	0.79345	0.76638	0.76857	0.78203	0.78284	0.84980
OzNet	0.77364	0.80101	0.77364	0.77364	0.78721	0.78820	0.87123
ResNet-50	0.92264	0.79849	0.80100	0.85752	0.85832	0.85657	0.94302
SqueezeNet	0.83668	0.82872	0.81111	0.8237	0.83269	0.83244	0.90630
VGG-16	0.81948	0.87909	0.85629	0.83748	0.84877	0.85121	0.92660

When we compare the performance of these architectures and OzNet in terms of the COVID-19 CT dataset processed with DWT, **we observe that pretty much each architecture's performance increases by comparison raw dataset results**. OzNet has very high-performance metrics: AUC, accuracy, sensitivity, specificity, precision and F1-score which are 99.9%, 99.5 %, 98.86%, 99.5%, 99.4% and 99.1% respectively. All performance metrics results are displayed in Table 5.

Table 5. Performance metrics of CNN architectures using the COVID-19 CT dataset processed with DWT

CNN Architectures	Performance Metrics						
	Sensitivity	**Specificity**	**Precision**	**F1-Score**	**G-Mean**	**Accuracy**	**AUC**
AlexNet	0.98567	0.98741	0.98570	0.98567	0.98650	0.9866	0.99960
DenseNet201	1.00	0.99244	0.99150	0.99572	0.99620	0.99598	0.99997
GoogleNet	0.99714	0.99496	0.99430	0.99571	0.99610	0.99598	0.99996
NASNetMobile	0.99140	0.98237	0.98020	0.98575	0.98690	0.9866	0.99330
OzNet	0.98860	0.99496	0.99430	0.99138	0.99175	0.99496	0.99985
ResNet-50	1.00	0.99496	0.99430	0.99714	0.99748	0.99732	0.99997
SqueezeNet	1.00	0.99496	0.99430	0.99714	0.99748	0.99732	0.99997
VGG-16	1.00	0.99496	0.99430	0.99714	0.99748	0.99732	0.99997

When we investigate the performance of these architectures in terms of the COVID-19 CT dataset processed with the intensity adjustment by comparison raw dataset results, we view that each architecture's performance is neither good nor bad. Actually, we can say that this pre-processing method does not increase architectures' classification success. In this case, the best-performing architecture is DenseNet201 with an accuracy of 85.7 %. Additionally, OzNet has AUC, accuracy, sensitivity, specificity, precision and F1-score which are 86.29%,77.48 %,73.93%, 80.6%, 77.01% and 75.44% respectively. All performance metrics results are exhibited in Table 6.

Table 6. Performance metrics of CNN architectures using the COVID-19 CT dataset processed with the intensity adjustment

CNN Architectures	Performance Metrics						
	Sensitivity	**Specificity**	**Precision**	**F1-Score**	**G-Mean**	**Accuracy**	**AUC**
AlexNet	0.76791	0.72544	0.71087	0.73829	0.74637	0.74531	0.82719
DenseNet201	0.92550	0.79849	0.80149	0.85904	0.85965	0.85791	0.94082
GoogleNet	0.74785	0.82872	0.79331	0.76991	0.78725	0.79088	0.86680
NASNetMobile	0.79656	0.74811	0.73545	0.76479	0.77196	0.77078	0.84150
OzNet	0.73926	0.80605	0.77015	0.75439	0.77193	0.77480	0.86288
ResNet-50	0.95129	0.68010	0.72331	0.82178	0.80435	0.80697	0.92020
SqueezeNet	0.81662	0.77582	0.76203	0.78838	0.79596	0.79491	0.87740
VGG-16	0.87679	0.80101	0.79481	0.83379	0.83804	0.83646	0.92493

When we examine the performance of these architectures in terms of the COVID-19 CT dataset transformed from gray to color RGB, by comparison, raw dataset results, we observe that each architecture's performance is also neither good nor bad. Essentially, we expect that the transformation that increased the discrimination with the human eye would have a positive

effect on the machine as well. However, we can state that these transformation architectures neither increase nor decrease the classification success nearly. In this instance, the best-performing architecture has DenseNet201 with an accuracy of 84.85 % again. Further, OzNet has AUC, accuracy, sensitivity, specificity, precision and F1-score which are 85.97%,77.74 %,75.93%, 79.34%, 76.37% and 77.62% respectively. All performance metrics results are demonstrated in Table 7.

Table 7. Performance metrics of CNN architectures using the COVID-19 CT dataset processed with gray to color RGB conversion.

CNN Architectures	Performance Metrics						
	Sensitivity	**Specificity**	**Precision**	**F1-Score**	**G-Mean**	**Accuracy**	**AUC**
AlexNet	0.77937	0.76574	0.74521	0.76191	0.77253	0.77212	0.84573
DenseNet201	0.92264	0.78337	0.78922	0.85073	0.85016	0.84853	0.93932
GoogleNet	0.80229	0.80856	0.78652	0.79433	0.80542	0.80563	0.88880
NASNetMobile	0.79943	0.75567	0.74202	0.76966	0.77724	0.77614	0.83580
OzNet	0.75931	0.79345	0.76369	0.76149	0.77619	0.77748	0.85970
ResNet-50	0.91117	0.76071	0.76998	0.83465	0.83255	0.83110	0.92880
SqueezeNet	0.83954	0.78338	0.77309	0.80495	0.81097	0.80965	0.89740
VGG-16	0.85387	0.81108	0.79893	0.82548	0.83220	0.83110	0.92380

Based on all these results, we can express that both processing methods do not raise the performance of these architectures. Essentially, many researchers discuss whether preprocessing is necessary for CNN architectures. However, after the DWT processing, all used architecture achieved high classification success in our study. Thus, this study shows that DWT processing is a very effective pre-processing method. In addition, in this study, we presented a 34-layers deep learning architecture, which has a very high classification success and takes its place among other pre-trained architectures and is called as OzNet. This architecture not only used just this study, but also another study. In one of study, OzNet achieved an accuracy of 95.6% [39], another study has achieved high accuracy. Fig.8 and Table 3 show details of OzNet. Of course, we do not show the classification success only on the performance metrics tables. We also show the confusion matrix on different preprocessed datasets in Fig.10. Besides, we display a histogram graph of performance metrics for different CT scan datasets for OzNet in Fig.11. Moreover, Fig.12 exhibits ROC curves and AUC values on different CT scan datasets for OzNet.

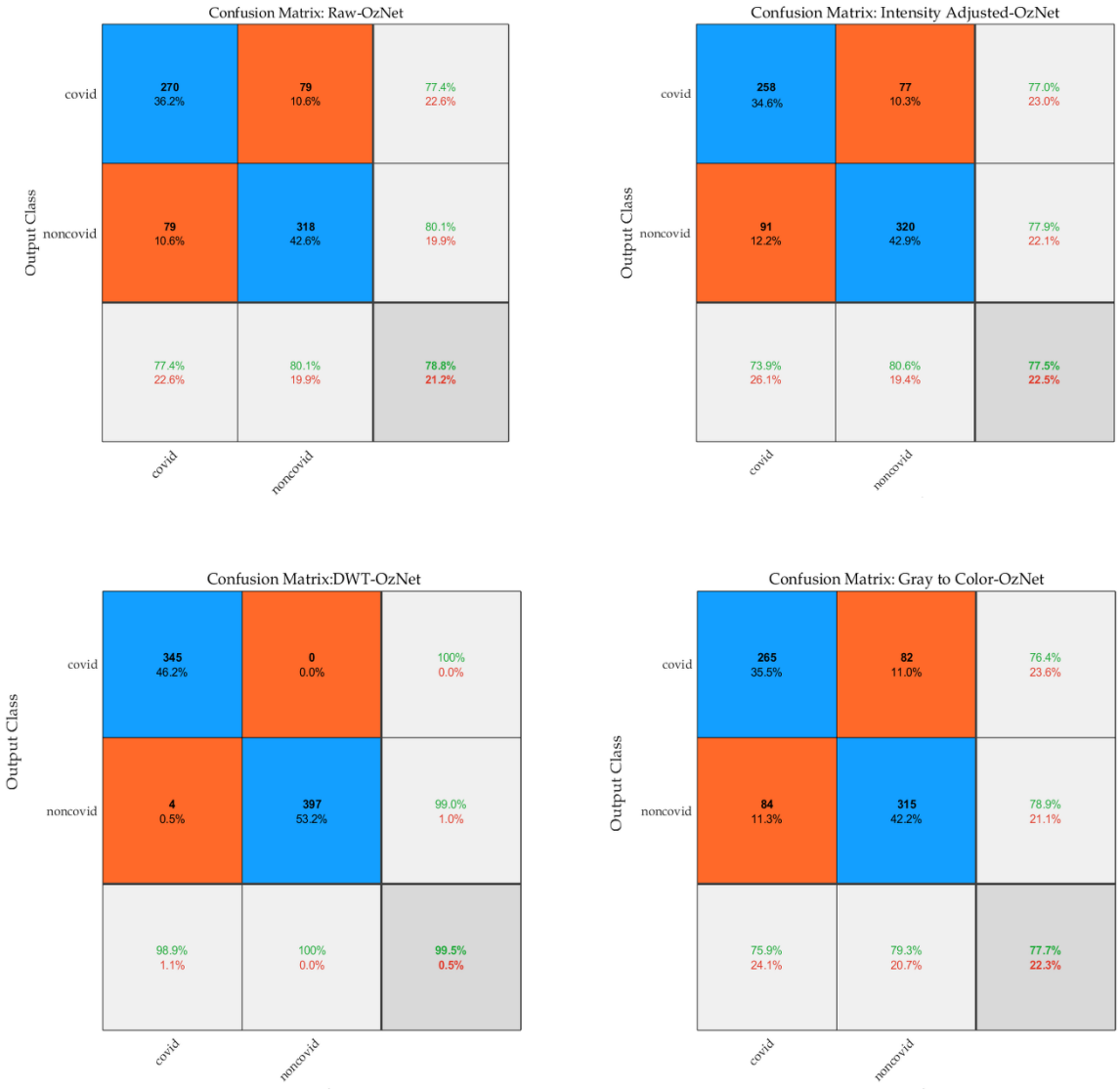

Fig.10. OzNet confusion matrix for different preprocessed CT scan datasets

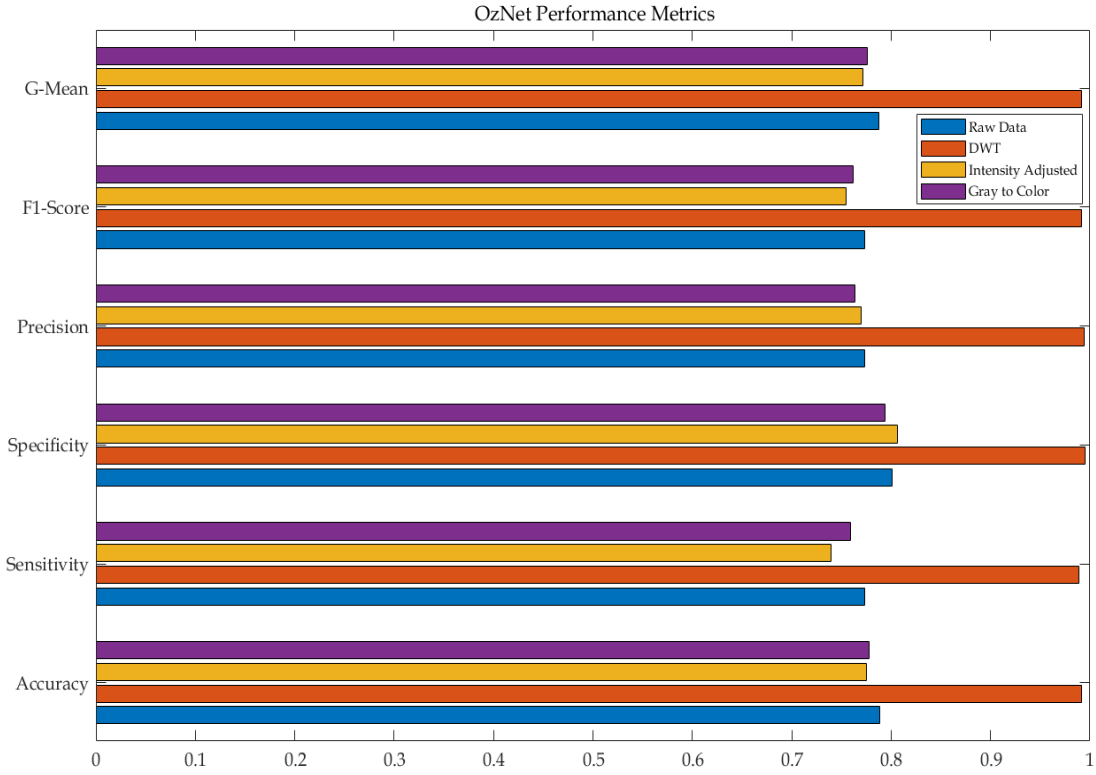

Fig.11. Performance of OzNet model for different CT scans.

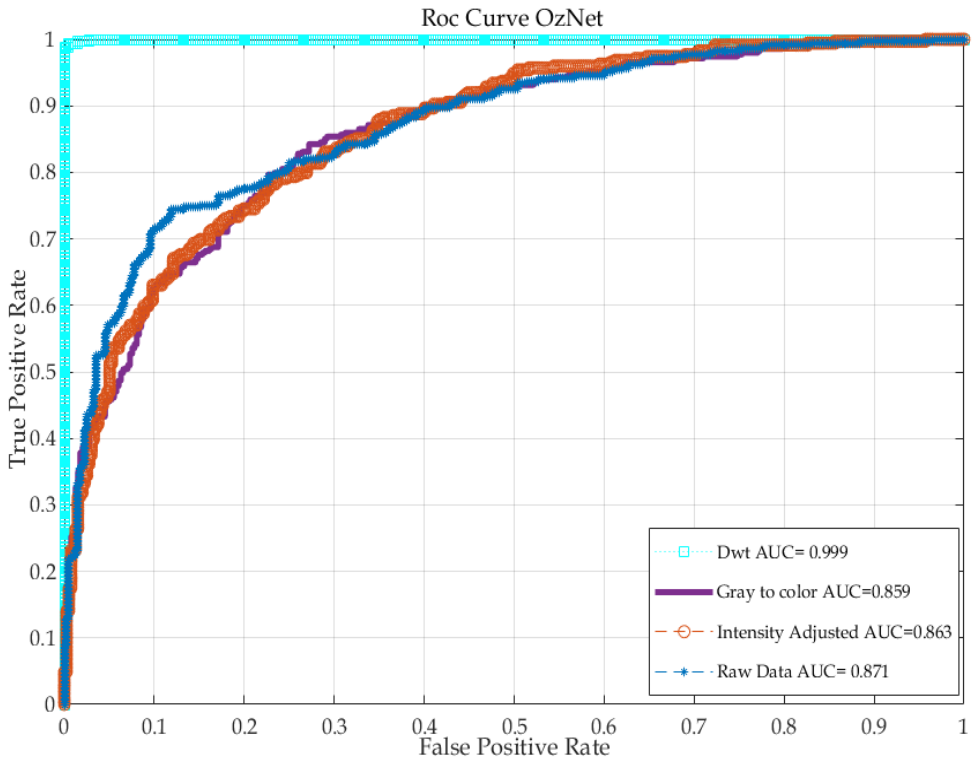

Fig.12. ROC curves of OzNet for different CT scans

3.3.Limitations of the study

In this part, we present the limitations of the proposed DWT-OzNet hybrid algorithm. Firstly, the datasets contained limited CT scans. Additionally, more expanded results may be obtained from Chest X-ray images when DWT-CNN algorithms are used. In this study, we applied single-level decomposing via the symmetric extension (sym) function. For the next studies, high-level decomposing with the same or different wavelet function can be used when implementing DWT to images.

3.4.Discussion

Discrete wavelet transform (DWT) for image processing is very popular method for image compression, image reduction, image optimization, and image watermark [56]. Many researchers consider that image compression reduces the quality of images, and this method may lose some information on images. However, while DWT is reducing size of images, it is not losing the quality of images [57]. Therefore, it is very effective to utilize this transform when it comes to health. Additionally, this study indicates that DWT is a powerful pre-processing method with CNN architectures for classifying CT scans datasets. In Table 5, the performance metrics are presented for the success of this pre-processing method. Moreover, we develop a novel deep learning algorithm, called as OzNet, which is compared with the widely known pre-trained architectures. It is known that the success of these pre-trained architectures has been proven and tried over and over again. Further, the success of our proposed architecture, Oznet, succeeds in being among these architectures. Clearly, we can say that DWT-Oznet approach is achieved good results in terms of performance metrics. Also, In Table 8, the comparison of the proposed model with previous studies.

Table 8. Comparison of DWT-OzNet model with previous studies.

Study	**Data type**	**Classification Method**	**Metrics**
Goel et al. [58]	CT scan images	Hybrid Deep Learning Algorithm	97.78% Accuracy 97.77% F1-Score 97.78% Sensitivity
Irfan et al.[59]	CT scan images	Hybrid Deep Neural Networks	99% Accuracy
Acar et al. [60]	CT scan images	InceptionV3 with Generative Adversarial Network (GAN) InceptionV3 without GAN	99.51% Accuracy 99.5% F1-Score 99.13% Sensitivity 98.93% Accuracy 98.78% F1-Score 98.50% Sensitivity
Elmuogy et al. [61]	CT scan images	VGG-19	99.05% Accuracy 98.90% F1-Score 99.12% Sensitivity
Polsinelli et al. [62]	CT scan images	CNN architecture	85.03% Accuracy 86.20% F1-Score 87.55% Sensitivity
Kundu et al. [63]	CT scan images	CNN architecture	98.80% Accuracy 98.80% F1-Score 98.79% Sensitivity

Pathak et al. [64]	CT scan images	CNN architecture	93.02% Accuracy
Hasan et al. [65]	CT scan images	CNN architecture	92% Accuracy
Ozyurt et al.[66]	CT scan images	Deep Neural Networks ANN	95.84% Accuracy 95.83% F1-Score 95.76% G-Mean 94.10% Accuracy 94.08% F1-Score 94.06% G-Mean
Saad et al. [30]	CT scan images	CNN architecture based on image segmentation	98.90% Accuracy 98.92% F1-Score 98.50% Sensitivity
Song et al.[67]	CT scan images	CNN architecture	86% Accuracy
Loey et al. [68]	CT scan images	CNN architecture	82.91% Accuracy
Lu et al.[69]	CT scan images	CNN architecture	99.05% Accuracy 99.04% F1-Score 99.76% Sensitivity
Kaur and Gandhi [70]	CT scan images	Hybrid Deep Learning Algorithm	99.38% Accuracy 99.40% F1-Score 99.20% Sensitivity
This Study	**CT scan images**	**DWT-OzNet**	**99.5% Accuracy** **99.14% F1-Score** **98.86% Sensitivity**

4. Conclusions

In this study, we create a novel deep CNN architecture which has 34 layers with pre-processed CT scans of COVID-19. Besides, we compare developed OzNet with pre-trained architectures such as AlexNet, DenseNet201, GoogleNet, NASNetMobile, ResNet-50, SqueezeNet, and VGG-16, for raw-CT scans and pre-processed-CT scans of COVID-19. Then, 10-fold cross-validation is applied for the classification of raw-CT scans and pre-processed-CT scans. Thus, we ensure robust and reliable results. When the results of many studies are examined, it is seen that there are serious differences between the metrics. This is due to the imbalance in the data set. To avoid this situation as well as data overfitting, we implement data augmentation. Thus, we acquire the overall (10-fold) performance metrics for each used architecture, detailed in Table 3, Table 4, Table 5, and Table 6. Besides, we utilize three pre-processing methods, which are DWT, intensity adjustment, and gray to color RGB conversion. When we compare the performance of these architectures on the CT scans of COVID-19 processed with the DWT, we realize that the performance of the architectures improved with a certain amount. In this condition, OzNet architecture obtain with an average accuracy of 99.5%. Other performance metrics are AUC, sensitivity, specificity, precision and F1-score which are 99.9%, 98.86%, 99.5%, 99.4% and 99.1% respectively.

When we utilize the intensity adjustment method, we take the value of gamma as 2 namely darkness. The reason we get the gamma value of 2 is that we want the comparison to be more specific. Besides, when we compare the performance of these architectures on the CT

scans of COVID-19 processed with the intensity adjustment, we see that the performance of the architectures does not increase, according to the raw dataset.

We employ the min-max normalization method, in order to denoise the CT scans. Not only we denoise the images but also transform it from gray to color RGB data using purple color. If we want to express why we prefer to use this transformation, in theory, color images can be easily distinguished with the eye. We assume that it may be the same for machines as well. But the results are not as expected. We can say that the results are not better than the raw data.

The Discrete Wavelet Transform (DWT) is one of the most powerful preprocessing methods. As a result, we can express that the results improve much more using the power of the Discrete Wavelet Transform. Although pre-processing methods are avoided, we strongly recommend DWT, especially for CNN architectures. In brief, we propose the DWT-OzNet hybrid algorithm for classifying COVID-19 CT scan images.

In this study, a novel DWT-OzNet hybrid algorithm is developed for COVID-19 detection using CT scan images to classify patients, automatically. Thus, clinicians will not consume much more time detecting COVID-19. In other words, the proposed hybrid algorithm can be utilized and expanded to detect COVID-19 in a clinical environment. In future work, we will apply the proposed hybrid algorithm to diverse medical datasets to control the correctness of this algorithm. We intend to gather real datasets such as MRI, X-ray, or CT scan images, and next detect special diseases by using OzNet and the proposed hybrid algorithm.

References

[1] W. H. Organization. https://covid19.who.int/ (accessed 30.04.2021 15:19.

[2] S.-H. Wang, V. V. Govindaraj, J. M. Górriz, X. Zhang, and Y.-D. Zhang, "Covid-19 classification by FGCNet with deep feature fusion from graph convolutional network and convolutional neural network," *Information Fusion,* vol. 67, pp. 208-229, 2021.

[3] M. F. Aslan, M. F. Unlersen, K. Sabanci, and A. Durdu, "CNN-based transfer learning–BiLSTM network: A novel approach for COVID-19 infection detection," *Applied Soft Computing,* vol. 98, p. 106912, 2021.

[4] S. R. Nayak, D. R. Nayak, U. Sinha, V. Arora, and R. B. Pachori, "Application of deep learning techniques for detection of COVID-19 cases using chest X-ray images: A comprehensive study," *Biomedical Signal Processing and Control,* vol. 64, p. 102365, 2021.

[5] X. Yang, X. He, J. Zhao, Y. Zhang, S. Zhang, and P. Xie, "COVID-CT-dataset: a CT scan dataset about COVID-19," *arXiv preprint arXiv:2003.13865,* 2020.

[6] R. Babukarthik, V. A. K. Adiga, G. Sambasivam, D. Chandramohan, and J. Amudhavel, "Prediction of covid-19 using genetic deep learning convolutional neural network (GDCNN)," *IEEE Access,* vol. 8, pp. 177647-177666, 2020.

[7] D.-P. Fan *et al.*, "Inf-net: Automatic covid-19 lung infection segmentation from ct images," *IEEE Transactions on Medical Imaging,* vol. 39, no. 8, pp. 2626-2637, 2020.

[8] D. Sharifrazi *et al.*, "Fusion of convolution neural network, support vector machine and Sobel filter for accurate detection of COVID-19 patients using X-ray images," *Biomedical Signal Processing and Control,* vol. 68, p. 102622, 2021.

[9] A. Subasi, A. Mitra, F. Ozyurt, and T. Tuncer, "Automated COVID-19 Detection from CT Images Using Deep Learning," in *Computer-aided Design and Diagnosis Methods for Biomedical Applications*: CRC Press, 2021, pp. 153-176.

[10] M. Barstugan, U. Ozkaya, and S. Ozturk, "Coronavirus (covid-19) classification using ct images by machine learning methods," *arXiv preprint arXiv:2003.09424*, 2020.

[11] S. H. Khan, A. Sohail, A. Khan, and Y. S. Lee, "Classification and region analysis of COVID-19 infection using lung CT images and deep convolutional neural networks," *arXiv preprint arXiv:2009.08864*, 2020.

[12] C. de Vente *et al.*, "Improving automated covid-19 grading with convolutional neural networks in computed tomography scans: An ablation study," *arXiv preprint arXiv:2009.09725*, 2020.

[13] T. D. Pham, "A comprehensive study on classification of COVID-19 on computed tomography with pretrained convolutional neural networks," *Scientific reports*, vol. 10, no. 1, pp. 1-8, 2020.

[14] O. A. Adebisi, J. A. Ojo, and O. M. Oni, "Comparative Analysis of Deep Learning Models for Detection of COVID-19 from chest X-Ray Images," *Int. J. Sci. Res. in Computer Science and Engineering Vol*, vol. 8, no. 5, 2020.

[15] M. A. Gungor, "A comparative study on wavelet denoising for high noisy CT images of COVID-19 disease," *Optik*, vol. 235, p. 166652, 2021.

[16] Y. S. Taspinar, I. Cinar, and M. Koklu, "Classification by a stacking model using CNN features for COVID-19 infection diagnosis," *Journal of X-Ray Science and Technology*, no. Preprint, pp. 1-16.

[17] A. Subasi, S. A. Qureshi, T. Brahimi, and A. Serireti, "COVID-19 detection from X-ray images using artificial intelligence," in *Artificial Intelligence and Big Data Analytics for Smart Healthcare*: Elsevier, 2021, pp. 209-224.

[18] G. Jia, H.-K. Lam, and Y. Xu, "Classification of COVID-19 chest X-Ray and CT images using a type of dynamic CNN modification method," *Computers in biology and medicine*, vol. 134, p. 104425, 2021.

[19] S. Thakur and A. Kumar, "X-ray and CT-scan-based automated detection and classification of covid-19 using convolutional neural networks (CNN)," *Biomedical Signal Processing and Control*, vol. 69, p. 102920, 2021.

[20] A. Narin, C. Kaya, and Z. Pamuk, "Automatic detection of coronavirus disease (covid-19) using x-ray images and deep convolutional neural networks," *Pattern Analysis and Applications*, pp. 1-14, 2021.

[21] S. Ahuja, B. K. Panigrahi, N. Dey, V. Rajinikanth, and T. K. Gandhi, "Deep transfer learning-based automated detection of COVID-19 from lung CT scan slices," *Applied Intelligence*, vol. 51, no. 1, pp. 571-585, 2021.

[22] T. Akram *et al.*, "A novel framework for rapid diagnosis of COVID-19 on computed tomography scans," *Pattern analysis and applications*, pp. 1-14, 2021.

[23] Y. Li, X. Pei, and Y. Guo, "A 3D CNN Classification Model for Accurate Diagnosis of Coronavirus Disease 2019 using Computed Tomography Images," *medRxiv*, 2021.

[24] T. Tuncer, F. Ozyurt, S. Dogan, and A. Subasi, "A novel Covid-19 and pneumonia classification method based on F-transform," *Chemometrics and Intelligent Laboratory Systems*, vol. 210, p. 104256, 2021.

[25] I. Ozsahin, B. Sekeroglu, M. S. Musa, M. T. Mustapha, and D. Uzun Ozsahin, "Review on diagnosis of COVID-19 from chest CT images using artificial intelligence," *Computational and Mathematical Methods in Medicine*, vol. 2020, 2020.

[26] M. Gour and S. Jain, "Uncertainty-aware convolutional neural network for COVID-19 X-ray images classification," *Computers in biology and medicine*, vol. 140, p. 105047, 2022.

[27] A. K. Dash and P. Mohapatra, "A Fine-tuned deep convolutional neural network for chest radiography image classification on COVID-19 cases," *Multimedia Tools and Applications,* vol. 81, no. 1, pp. 1055-1075, 2022.
[28] S. Chakraborty, S. Paul, and K. Hasan, "A transfer learning-based approach with deep cnn for covid-19-and pneumonia-affected chest x-ray image classification," *SN Computer Science,* vol. 3, no. 1, pp. 1-10, 2022.
[29] M. F. Aslan, K. Sabanci, A. Durdu, and M. F. Unlersen, "COVID-19 diagnosis using state-of-the-art CNN architecture features and Bayesian Optimization," *Computers in Biology and Medicine,* p. 105244, 2022.
[30] W. Saad, W. A. Shalaby, M. Shokair, F. A. El-Samie, M. Dessouky, and E. Abdellatef, "COVID-19 classification using deep feature concatenation technique," *Journal of Ambient Intelligence and Humanized Computing,* vol. 13, no. 4, pp. 2025-2043, 2022.
[31] J. Amin, M. A. Anjum, M. Sharif, A. Rehman, T. Saba, and R. Zahra, "Microscopic segmentation and classification of COVID-19 infection with ensemble convolutional neural network," *Microscopy research and technique,* vol. 85, no. 1, pp. 385-397, 2022.
[32] A. Krizhevsky, I. Sutskever, and G. E. Hinton, "Imagenet classification with deep convolutional neural networks," *Advances in neural information processing systems,* vol. 25, pp. 1097-1105, 2012.
[33] G. Huang, Z. Liu, L. Van Der Maaten, and K. Q. Weinberger, "Densely connected convolutional networks," in *Proceedings of the IEEE conference on computer vision and pattern recognition*, 2017, pp. 4700-4708.
[34] C. Szegedy *et al.*, "Going deeper with convolutions," in *Proceedings of the IEEE conference on computer vision and pattern recognition*, 2015, pp. 1-9.
[35] B. Zoph, V. Vasudevan, J. Shlens, and Q. V. Le, "Learning transferable architectures for scalable image recognition," in *Proceedings of the IEEE conference on computer vision and pattern recognition*, 2018, pp. 8697-8710.
[36] K. He, X. Zhang, S. Ren, and J. Sun, "Deep residual learning for image recognition," in *Proceedings of the IEEE conference on computer vision and pattern recognition*, 2016, pp. 770-778.
[37] F. N. Iandola, S. Han, M. W. Moskewicz, K. Ashraf, W. J. Dally, and K. Keutzer, "SqueezeNet: AlexNet-level accuracy with 50x fewer parameters and< 0.5 MB model size," *arXiv preprint arXiv:1602.07360,* 2016.
[38] K. Simonyan and A. Zisserman, "Very deep convolutional networks for large-scale image recognition," *arXiv preprint arXiv:1409.1556,* 2014.
[39] Ö. Özaltın and Ö. Yeniay, "ECG Classification Performing Feature Extraction Automatically Using a Hybrid CNN-SVM Algorithm," in *2021 3rd International Congress on Human-Computer Interaction, Optimization and Robotic Applications (HORA)*, 2021: IEEE, pp. 1-5.
[40] S. Jkooy. https://github.com/UCSD-AI4H/COVID-CT (accessed 03.03.2021 15:57.
[41] A. Sarhan, "Run length encoding based wavelet features for COVID-19 detection in X-rays," *BJR| Open,* vol. 3, no. 1, p. 20200028, 2021.
[42] İ. V. Öner, M. K. Yeşilyurt, and E. Ç. YILMAZ, "WAVELET ANALİZ TEKNİĞİ VE UYGULAMA ALANLARI," *Ordu Üniversitesi Bilim ve Teknoloji Dergisi,* vol. 7, no. 1, pp. 42-56, 2017.
[43] J. Amin, M. Sharif, N. Gul, M. Yasmin, and S. A. Shad, "Brain tumor classification based on DWT fusion of MRI sequences using convolutional neural network," *Pattern Recognition Letters,* vol. 129, pp. 115-122, 2020.
[44] H. Khorrami and M. Moavenian, "A comparative study of DWT, CWT and DCT transformations in ECG arrhythmias classification," *Expert systems with Applications,* vol. 37, no. 8, pp. 5751-5757, 2010.

[45] I. Krak, O. Stelia, A. Pashko, M. Efremov, and O. Khorozov, "Electrocardiogram Classification Using Wavelet Transformations," in *2020 IEEE 15th International Conference on Advanced Trends in Radioelectronics, Telecommunications and Computer Engineering (TCSET)*, 2020: IEEE, pp. 930-933.

[46] R. D. Pai, S. Halvi, and B. Hiremath, "Medical color image enhancement using wavelet transform and contrast stretching technique," *International Journal of Scientific and Research Publications*, vol. 5, no. 7, pp. 1-7, 2015.

[47] P. Rajan and C. Sundar, "Brain tumor detection and segmentation by intensity adjustment," *Journal of medical systems*, vol. 43, no. 8, pp. 1-13, 2019.

[48] H. Lin, J. Gao, Q. Mei, G. Zhang, Y. He, and X. Chen, "Three-dimensional shape measurement technique for shiny surfaces by adaptive pixel-wise projection intensity adjustment," *Optics and Lasers in Engineering*, vol. 91, pp. 206-215, 2017.

[49] A.-W. S. Ibrahim and H. J. Sartep, "Grayscale image coloring by using YCbCr and HSV color spaces," *compare*, vol. 4, no. 4, 2017.

[50] H. Kekre, S. D. Thepade, A. Athawale, and A. Parkar, "Using assorted color spaces and pixel window sizes for colorization of grayscale images," in *Proceedings of the International Conference and Workshop on Emerging Trends in Technology*, 2010, pp. 481-486.

[51] Y. LeCun *et al.*, "Learning algorithms for classification: A comparison on handwritten digit recognition," *Neural networks: the statistical mechanics perspective*, vol. 261, no. 276, p. 2, 1995.

[52] S. K. Addagarla, G. K. Chakravarthi, and P. Anitha, "Real time multi-scale facial mask detection and classification using deep transfer learning techniques," *International Journal*, vol. 9, no. 4, pp. 4402-4408, 2020.

[53] A. L. Goldberger *et al.*, "PhysioBank, PhysioToolkit, and PhysioNet: components of a new research resource for complex physiologic signals," *circulation*, vol. 101, no. 23, pp. e215-e220, 2000.

[54] M. Koklu and I. A. Ozkan, "Multiclass classification of dry beans using computer vision and machine learning techniques," *Computers and Electronics in Agriculture*, vol. 174, p. 105507, 2020.

[55] S. Arlot and A. Celisse, "A survey of cross-validation procedures for model selection," *Statistics surveys*, vol. 4, pp. 40-79, 2010.

[56] G. Othman and D. Q. Zeebaree, "The applications of discrete wavelet transform in image processing: A review," *Journal of Soft Computing and Data Mining*, vol. 1, no. 2, pp. 31-43, 2020.

[57] A. Katharotiya, S. Patel, and M. Goyani, "Comparative analysis between DCT & DWT techniques of image compression," *Journal of information engineering and applications*, vol. 1, no. 2, pp. 9-17, 2011.

[58] C. Goel, A. Kumar, S. K. Dubey, and V. Srivastava, "Efficient deep network architecture for covid-19 detection using computed tomography images," *medRxiv*, 2020.

[59] M. Irfan *et al.*, "Role of Hybrid Deep Neural Networks (HDNNs), Computed Tomography, and Chest X-rays for the Detection of COVID-19," *International Journal of Environmental Research and Public Health*, vol. 18, no. 6, p. 3056, 2021.

[60] E. Acar, E. Şahin, and İ. Yilmaz, "Improving effectiveness of different deep learning-based models for detecting COVID-19 from computed tomography (CT) images," *medRxiv*, 2020.

[61] S. Elmuogy, N. A. Hikal, and E. Hassan, "An efficient technique for CT scan images classification of COVID-19," *Journal of Intelligent & Fuzzy Systems*, vol. 40, no. 3, pp. 5225-5238, 2021.

[62] M. Polsinelli, L. Cinque, and G. Placidi, "A light CNN for detecting COVID-19 from CT scans of the chest," *Pattern recognition letters,* vol. 140, pp. 95-100, 2020.
[63] R. Kundu, H. Basak, P. K. Singh, A. Ahmadian, M. Ferrara, and R. Sarkar, "Fuzzy rank-based fusion of CNN models using Gompertz function for screening COVID-19 CT-scans," *Scientific reports,* vol. 11, no. 1, pp. 1-12, 2021.
[64] Y. Pathak, P. K. Shukla, A. Tiwari, S. Stalin, and S. Singh, "Deep transfer learning based classification model for COVID-19 disease," *Irbm,* 2020.
[65] N. Hasan, Y. Bao, and A. Shawon, "DenseNet convolutional neural networks application for predicting COVID-19 using CT image," 2020.
[66] F. Ozyurt, T. Tuncer, and A. Subasi, "An automated COVID-19 detection based on fused dynamic exemplar pyramid feature extraction and hybrid feature selection using deep learning," *Computers in Biology and Medicine,* vol. 132, p. 104356, 2021.
[67] Y. Song *et al.*, "Deep learning enables accurate diagnosis of novel coronavirus (COVID-19) with CT images," *IEEE/ACM Transactions on Computational Biology and Bioinformatics,* 2021.
[68] M. Loey, G. Manogaran, and N. E. M. Khalifa, "A deep transfer learning model with classical data augmentation and cgan to detect covid-19 from chest ct radiography digital images," *Neural Computing and Applications,* pp. 1-13, 2020.
[69] S. Lu, Z. Zhu, J. M. Gorriz, S. H. Wang, and Y. D. Zhang, "NAGNN: classification of COVID-19 based on neighboring aware representation from deep graph neural network," *International Journal of Intelligent Systems,* vol. 37, no. 2, pp. 1572-1598, 2022.
[70] T. Kaur and T. K. Gandhi, "Classifier fusion for detection of COVID-19 from CT scans," *Circuits, systems, and signal processing,* vol. 41, no. 6, pp. 3397-3414, 2022.